“Plasma Assisted Synthesis of Molybdenum Carbide Catalyst”

REUs: Llarimar Maldonado-Rodriguez and Pamela Buzzetta
RET: Timothy Walsh
Graduate Student Advisor: Gabriel Duran
Faculty Advisor: Dr. Kenneth Brezinsky
5 August 2005

“Novel Materials and Processing in Chemical and Biomedical Engineering”
National Science Foundation - Research Experience for Undergraduates
University of Illinois at Chicago
Summer 2005
UIC Program Directors: Dr. Christos Takoudis and Dr. Andreas Linninger

1.0 Abstract

Carbide and nitride catalysts are becoming industrially significant catalysts. A scalable, inexpensive, and safe process is needed to produce these catalysts. We are developing a plasma-assisted synthesis via a glow plasma discharge to produce these catalysts. It operates at low temperatures and in an efficient manner. Characterizing a control process that considers all the parameters in the production of these catalysts is the major objective in this research. Providing the scientific community with experimental evidence of the mechanisms and behaviors is also essential.

This paper goes on to describe the background on carbide and nitride catalysts, theory of the plasma-assisted process and varying system parameters, experimental procedure for our methods, our analysis of the sample products using Raman Spectroscopy, X-ray Photoelectron Spectroscopy (XPS), and Scanning Electron Microscopy (SEM) instruments, the conclusions we were able to draw from the analysis, and future work based on the findings. In particular, we synthesized and studied the molybdenum carbide catalyst as it was the most competitive with industrial catalysts, as shown in previous studies. We started with a molybdenum wire or foil strip and then used the plasma discharge to react ethylene at the metal surface to create thin films. Analysis of the films showed varied concentrations of molybdenum oxides, carbides, oxycarbides, and carbon deposits on the samples. The parameters we varied and analyzed were: the duration of the reaction in the Plasma Discharge Reactor, the system pressure, and the gas source composition. All three specifications appeared to affect both the film composition and uniformity.

We could not definitively distinguish molybdenum carbide with the available tools of analysis, but future work with Transmission Electron Microscopy (TEM) to measure the crystal lattice spacing, in conjunction with our analyses, should confirm the film's components. We did identify molybdenum oxides and carbon deposits at the surface, which tells us that we can achieve surface reactions that are essential to creating the carbide and nitride films. Our pressure and reaction time variations demonstrated that optimal values exist that allow for film formation without degradation or large deposits of unwanted materials, such as the oxides and carbon graphite or diamond structures.

2.0 Table of Contents

3.0 Acknowledgments

We would like thank the National Science Foundation EEC-0453432 Grant that sponsored our 2005 Summer Research Experience for Undergraduates (REU) and our Research Experience for Teachers (RET) programs at the University of Illinois at Chicago. We recognize that this program would not have been in existence if it were not for the vision and leadership of the RET and REU site directors: Dr. Andreas Linninger and Dr. Christos Takoudis. We are indebted to your notion of public service and are appreciative of your efforts to promote science education.

Additionally, we would like to extend our gratitude to the following individuals for their individual contributions to our research project:

Gabriel Duran, thank you for allowing us to work on this project with you. We hope that the information in this report is useful to you in your future endeavors.

Professor Kenneth Brezinsky, we are sincerely grateful to have had the opportunity to work with you this summer. We admire your outlook on science and life, and have greatly benefitted from the many helpful conversations about our project.

Dr. Alexei Saveliev, thank you for your guidance and technical help in setting up the plasma reactor apparatus and keeping it running. The plethora of knowledge you shared with us in the plasma field was vital to our research. We would have been lost without you. We also greatly appreciate the lab space and resources you and Dr. Lawrence Kennedy so generously supplied.

Dr. John Roth, your willingness to share your analytical knowledge (and sometimes office space) to assist our research will not be forgotten.

Brian Schwandt, our project would have reached an impasse if it were not for your glassblowing skill. We also greatly appreciated your willingness to share your work with us and answer our sometimes difficult questions.

Dr. Jennifer Dunn, we were sorry to see you go so early in the summer, but are thankful for your assistance in getting us up to speed during the first two weeks of this project.

Charlie Robinson, thank you for your technical assistance in the laboratory.

We also thank MARC U*STAR PUCPR Honor Program for supporting Llary.

4.0 List of Figures and Tables

5.0 Introduction to Carbide and Nitride Catalysts

The increasing importance of carbide and nitride catalysts in industrial processes has produced a large field of research in their processing. However, most current processes are not conducive to large scale production. Our approach in plasma-assisted synthesis may be a viable solution to this issue and we provide an outline as to how we may reach that solution.

5.1 Motivation for Producing Carbide and Nitride Catalysts

Noble metal catalysts have become essential to a multitude of industrial projects. However, these resources are increasing in rarity to the point of concern. This has led to a desire for inexpensive alternatives. Our research approaches this dilemma by exploring the possibility of using carbide and nitride catalysts as a replacement.

Carbides and nitrides have several important characteristics that make them valuable to industry. These compounds mimic the properties of platinum[1,2] and have the potential to replace expensive and increasingly rare noble metal catalysts[1] (Pt, Pd, Ru, Rh) for several industrially significant reactions including hydrogenation[2,3], hydrogenolysis[2], methane activation[1,4], amination[23], acetone condensation[10], and isomerization[5] reactions. From 240 to 300°C, the CO consumption rate in the Water-Gas Shift (WGS) reaction, which generates H_2 for PEM fuel cells, was significantly higher for Mo_2C than for commercial Cu-Zn-Al[6,7]. Also, they have a tolerance for sulfur and nitrogen impurities[2,8]. This property makes them candidate catalysts for hydroprocessing[9], which produces cleaner burning hydrocarbon fuels.

5.2 Previous and Current Synthesis Techniques

The most common practices in creating carbide and nitride catalysts are mostly thermal processes such as thermal chemical vapor deposition (CVD), self-propagating high-temperature synthesis (SHS)[22,24], and temperature-programed reactions (TPR)[10,22]. Most of these are carburization reactions where the carbide replaces an initial metal oxide. In these, high temperatures are required to produce the thermal decomposition of

the desired species so that they become reactive[21] and allow the reaction to proceed that produces the catalyst. Many of these processes also entail long periods of ramped heating and then maintaining the high temperatures[22]. This becomes cumbersome and costly in terms of synthesis, which make industrial level upscaling of the procedures very difficult.

The technique previously used in our laboratory to address the issues with high temperature processes was the Microwave Assisted Fluidized Bed Synthesis (MAFBS). The MAFBS technique was used to create the metal powders because it reduces the processing time, costs, and energy consumption over conventional heating methods[11]. Additionally, the environment of a microwave-based process may be safer because exterior parts to the microwave oven do not become excessively hot[11]. However, during the use of the MAFBS, the morphology of the metal catalyst powders could not be controlled. Also, an arcing was observed in the reaction chamber and we hypothesize that it might be creating plasma that is responsible for the film formation. This led to the plasma-assisted process that we describe over the duration of this paper and use in our experimentation.

5.3 Objectives of the Plasma-Assisted Process

The main goals of our current project were to produce a molybdenum carbide film from pure molybdenum wire or foil and then assess the film properties based on parameter variations. To achieve these goals, we analyzed how the film's composition and uniformity were affected by reactor parameters such as: morphology of molybdenum base (whether we used wires or foil strips), gas phase composition, reaction duration, and pressure.

6.0 Theory of a Plasma-Assisted Synthesis

There are two scopes to explore within the theory of plasma-assisted catalyst synthesis. The first is the mechanism of reaction at the transitional metal surface, which could follow two possible routes: a deposition reaction called Plasma-Enhanced Chemical Vapor Deposition (PECVD) that creates a reactive gas species or a surface modification of the metal that allows the reaction between the reactive species and the

metal. A combination of the two mechanisms is also a plausible scenario. The second inquiry that we were able to investigate is how the system parameters may affect the catalyst's film characteristics.

6.1 PECVD and Surface Modification Theories

The first process that might have assisted in forming the film at the catalyst surface is PECVD. Our reactor used an electrode, comprised of an anode and cathode, over which a high voltage source was applied. The gas mixture containing the carbon source in a carrier gas flowed over the electrode. This allowed the cathode to emit electrons while particles and light quanta from the reactant gas bombarded the area to create glow plasma discharges[12]. The end result was the creation of highly reactive ions and radicals of the carbon based gas at the electrode walls. As the reactive species transported to the metal catalyst base, an array of absorptions and reactions may have taken place to form the films[13]. These reactions could produce surface deposition of the carbon species that we observed. Depositing carbon is not the desired process for creating a carbide layer; it requires a reaction at the metal surface that produces the new carbide species at the wire surface.

Since our metal substrates and gas source were simultaneously in contact with the plasma discharge, another explanation for the film formations could be that the plasma also modified the surface of the metal and allowed surface reactions to occur. This hopefully created the carbide layer that is essential to our catalysts synthesis. Plasma processing is a typical route to alter polymer surfaces and although it is not common to use it on metals and ceramics[14], it can create a reactive surface susceptible to the reactant gas. Another consideration is that the actual process could have been a coupling of PECVD using the gas phase and the surface modification using the metal's surface.

6.2 System Parameter Effects

There are many considerations to make in these catalyst syntheses that will affect the final product and ultimately, its utility to industry and science. The identity of the base catalyst or transitional metal and then the identity of the carbon or nitrogen source comprise the basis for the synthesis. Once these specifications are set, the reactor itself

has many parameters to vary. They all affect the ability of the carbide or nitride film to form and its consequent uniformity, thickness, and composition.

The parameters that can be considered within our reactor are: pressure, temperature, current supply, gas phase composition, and morphology of the molybdenum substrate. We did not explore every one of these in our project, but it will be essential to characterize all of these elements in future work to fully optimize the reactions at the metal surface. The pressure is actually coupled with the temperature in that raising the pressure will also increase temperatures in the reactor and vice versa. Higher temperatures will result in either case, which leads to an increase in the concentration of reactive species and could ultimately produce thicker films at faster rates. Increasing the current also increases the reactive species' concentrations because the number of electrons emitted from the cathode increases, which leads to a larger plasma. The reaction duration is hypothesized to create thicker films as more time is allowed for bombardment of the metal substrate by the reactant gas. The morphology of the metal base will most likely play a role in the degree of uniformity of the film coating[15]. A final note on these parameters is that we must consider that the amount of contaminants or undesired reactions creating carbon, nitrogen, and oxide deposits, which could also be changing with the desired film. The rest of the paper is dedicated to describing and analyzing the initial experimentation with a selection of these parameters.

7.0 Apparatus and Procedure for Catalyst Synthesis

Our experiments focused on the production of Mo_2C on wires and foil strips because Mo_2C was the most competitive with the industrial catalysts[11] and the available apparatus was most conducive to using wire and foil samples. The reactor parameters evaluated thus far are: duration of the reaction, reactor chamber pressure, gas phase composition, and the molybdenum sample's morphology. The following provides an explanation of the set-up and procedure in performing these experiments.

7.1 Materials for Experiments

The experimental set-up required 0.25mm diameter Mo wire (99.97%) from Sigma-Aldrich, 0.025mm thick Mo foil (99.95%) from Advent Research Materials Ltd.,

ethylene gas from Matheson Tri-Gas, hydrogen gas from BOC Gases, and argon gas from Airgases Inc. For reference data during the analysis, additional materials used were Mo_2C powder (-325 mesh) from Sigma, MoO_3 powder (99%) from Sigma, and Mo powder (99.8%) from Atlantic Equipment Engineers.

7.2 Plasma Discharge Apparatus Used to Perform Reaction

The deposition apparatus employed in the experiments was a Plasma Discharge Reactor (PDR), developed in the mechanical engineering department at the University of Illinois at Chicago[11]. Figure 1 is a picture of the actual apparatus. The reaction occurred in the 3" diameter quartz tube sitting vertically on the reactor's metal frame. The tube confined the gas mixtures in the plasma discharge during the film formation. It also contained the wire or foil sample, the cathode, and the anode.

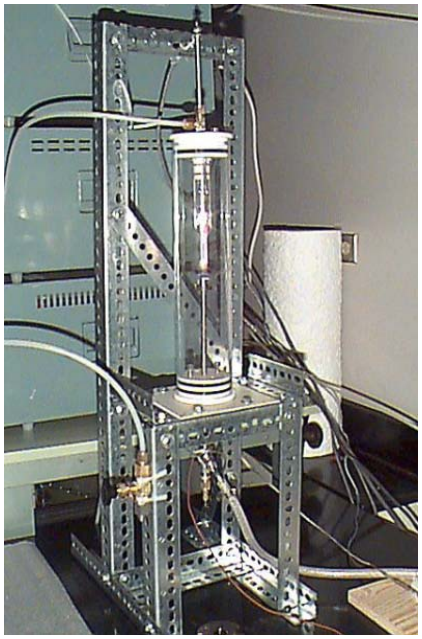

Figure 1: Plasma Discharge Reactor that performs the plasma-assisted catalyst synthesis

The high voltage supply connected at the anode that was held in place by a Teflon stopper at the top of the tube. The voltage supply first had to run through a resistor to stabilize the output and thus, the discharge. The ground wire was connected to the cathode plate that came up vertically from the bottom of the quartz tube through another

Teflon stopper. This completed the electrical circuit and created the plasma discharge between the anode and cathode when the system was running. A vacuum was also connected to the cathode plate that pulled the gases from the inlet at the anode through the bottom of the chamber. The flowmeter regulating the gases had lines running out to a mixing chamber to ensure an even distribution of ethylene in argon before going into the reaction chamber. The entire schematic is shown below in Figure 2.

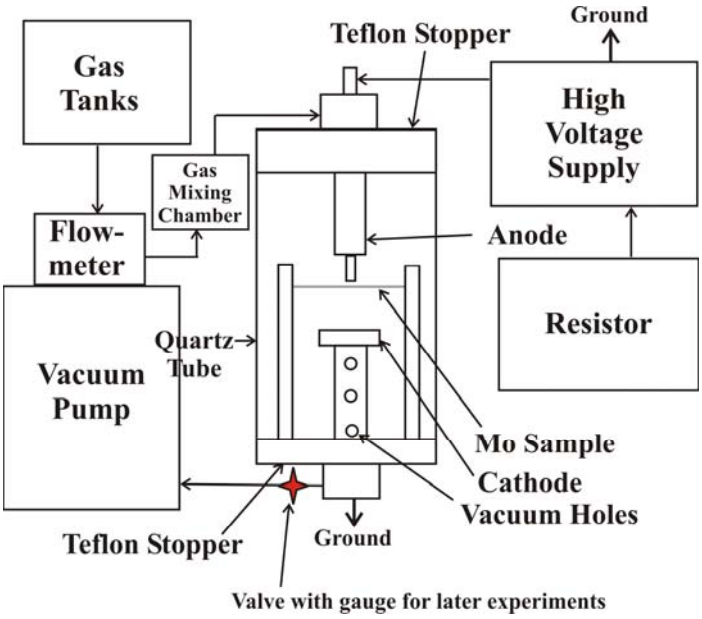

Figure 2: Schematic for experimental set-up

We made one alteration to the set-up during the course of our experiments that would allow us to vary the pressure in the quartz tube or reaction chamber. We added a valve and pressure gauge at the line between the vacuum pump and the bottom of the quartz tube. This is indicated by the red star in Figure 2.

7.3 Experimental Procedure and Development

The procedure began by equilibrating the flowmeter that controlled the gas flows from the tanks by turning it on for about 15 minutes before allowing any gas flow. A 2.5” long molybdenum wire or foil sample was stretched above the cathode plate so the wire was just below the glass tip of the anode, but not touching it, and then was centered

across the diameter of the cathode plate. Two metal posts with two nuts per post that screwed together were the anchors for the sample. The sample ends were secured between the two nuts. The quartz tube was placed over the molybdenum sample and electrode set-up, then the high voltage supply and gas line were connected. The gas tanks to the flowmeter were then opened and the high voltage supply, resistor, and vacuum were turned on. For the pressure variation experiments, the argon flow was opened to the reaction chamber at this point and then the valve was adjusted to the desired pressure. Then the argon was shut off and the PDR was ready to operate.

The plasma discharge had characteristic colors depending on the composition of the gas source. After the vacuum pumped the reaction chamber down to show about 10mbar of pressure in the system, a voltage potential of approximately 8.75 kV and current of about 80mA were applied across the electrode. 943 mL/min of Ar flow was opened at the flowmeter (which remained constant for every experiment as the carrier gas), which produced a columnated red plasma discharge as shown in Figure 3. The flow of C_2H_4 was then introduced to the reactor, which turned the discharge bright blue with a red tip (Figure 4). Turning off the C_2H_4 and introducing H_2 gas flow produced a darker bluish-purple discharge that was much less intense than the first two discharges (Figure 5). Timing began at the activation of either the ethylene or hydrogen flows, depending on the experiment parameters. After the wire modification, each sample was collected and stored in a glass vial until analysis.

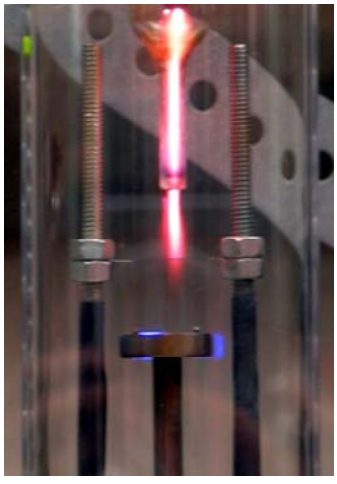

Figure 3: PDR plasma discharge in argon

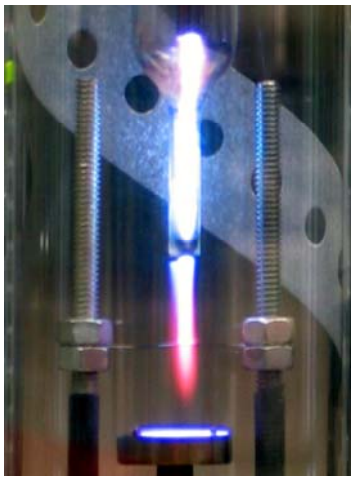

Figure 4: Discharge in ethylene-argon gas mixture

Figure 5: Discharge in hydrogen-argon gas mixture

The first problem we encountered in the original set-up was that we had a leak in the system. Many of our initial experiments were run with the vacuum showing almost 35mbar of pressure, rather than the 10mbar to which it would pump down after fixing the leak. This led to results that were not reproducible, so they were not valuable in terms of evaluating the carbide formation.

8.0 Results and Discussion of Catalyst Analyses

The three techniques of analysis that have been available thus far are Laser Raman Spectroscopy (LRS), X-ray Photoelectron Spectroscopy (XPS), and Scanning Electron Microscopy (SEM). The operation of the three instruments is briefly given and then the results that each produced for our samples is depicted and analyzed.

8.1 Raman Spectra of Sample Surfaces and Analysis

The Laser Raman Spectrometer works on the principle that a monochromatic laser beam irradiates a sample and the sample reflects scattered light because it doesn't absorb at the wavelength of the beam. The spectrum of the scattered radiation includes a line at this wavelength and a number of relatively weak bands at other wavelengths. The modified bands constitute the Laser Raman Spectrum (LRS) of the sample and are characteristic of the sample identity[16]. In particular, we used a Renishaw 2000

Ramascope, operating with an argon laser at 514.5nm, to observe alterations at the wire and foil sample surfaces. We compared our samples' spectra with a standard of MoO_3 and Mo powder and also with literature resources. According to the literature, the neither pure Mo nor Mo_2C produce a shift in the light source, but oxide and carbon deposits have distinct features[17,26,27]. Therefore, Raman was mainly used to identify the oxide and carbon deposit components or confirm that we had a clean sample of Mo if we were running reference samples.

The first sample analyzed here was created using a 250 μm Mo wire. It was run in the discharge with 943 mL/min Ar and 95 mL/min H_2 for 120 seconds; then we turned off the H_2 and allowed 10 mL/min of C_2H_4 flow in the Ar for 120 seconds. The C_2H_4 flow was then closed and the sample was kept in the discharge for an additional 60 seconds. The voltage was 8.77 kV and the current was 75 mA.

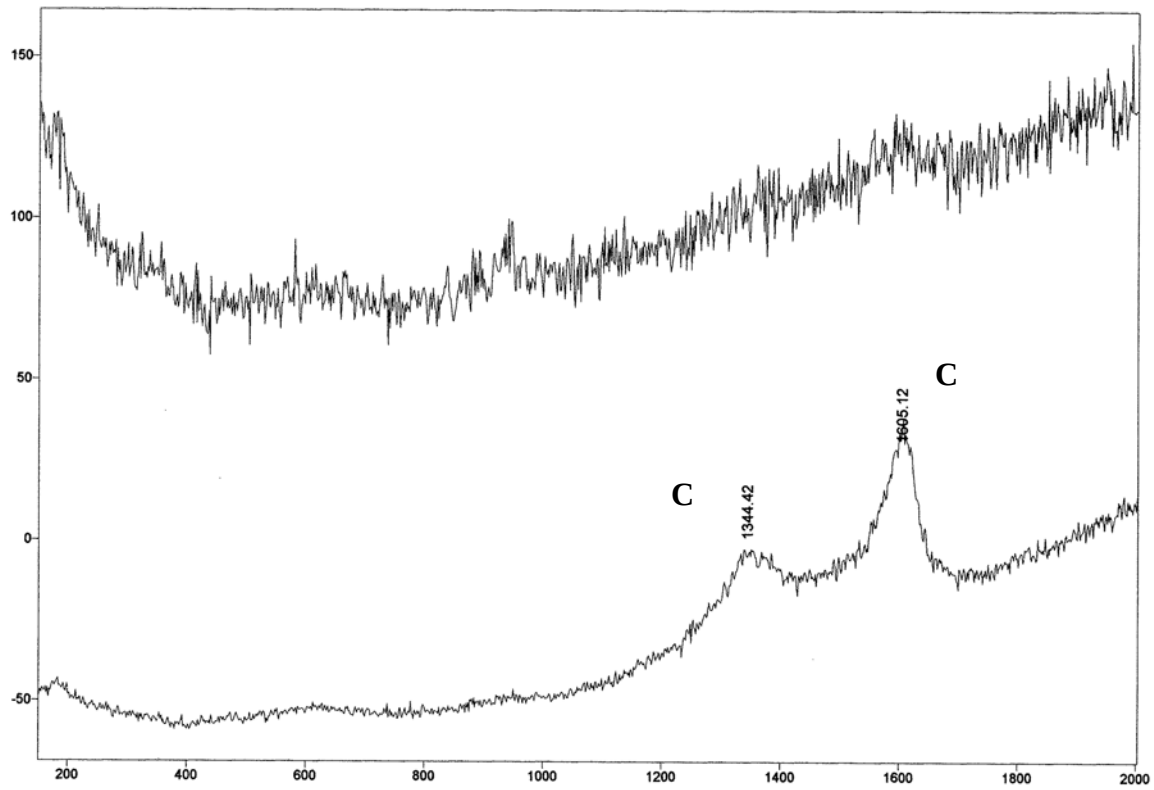

Figure 6: LRS for sample 1

Figure 6 has two lines, which represent the analysis of sample 1 in two different regions of the wire, producing two spectra. In the top spectrum, it is not possible to determine a peak. Therefore, an analysis of a second region was necessary, which is the bottom spectrum shown. In this second region, we see two main peaks at 1344 cm^{-1} and 1605 cm^{-1}. The 1344 cm^{-1} peak is attributed to the carbon-induced disorder at the D-line[17, 28, 29], and the 1605 cm^{-1} is attributed to carbon disorder[28, 29]. It is not possible to determine any molybdenum oxide peaks in this sample because the carbon deposit intensities were so high from their high concentrations that they may prevent detection of the oxides.

The second sample also used a 250 μm Mo wire. It was run with 943 mL/min of Ar and 95 mL/min of H_2 for 120 seconds. After removing the H_2 flow, 20.1 mL/min of C_2H_4 was immediately added for 120 seconds and then sample was kept only in the AR flow for 60 seconds. The voltage was 8.77 kV and the current was 75 mA.

Figure 7 on the next page is the Raman spectra of sample 2, where the wire was analyzed in three different regions, producing similar spectra with slight variations in the shifted frequencies. The peaks at 1342.35 cm^{-1}, 1352.7 cm^{-1}, and 1376 cm^{-1} are attributed to the carbon-induced disorder at the D-line[17, 28, 29]. The peaks at 1607.19 cm^{-1} and 1613.4 cm^{-1} are attributed to a carbon disorder at the G-line[28, 29]. Again, it is not possible to tell whether molybdenum oxides were formed with the Raman analysis on this sample from the high concentrations of carbon deposits.

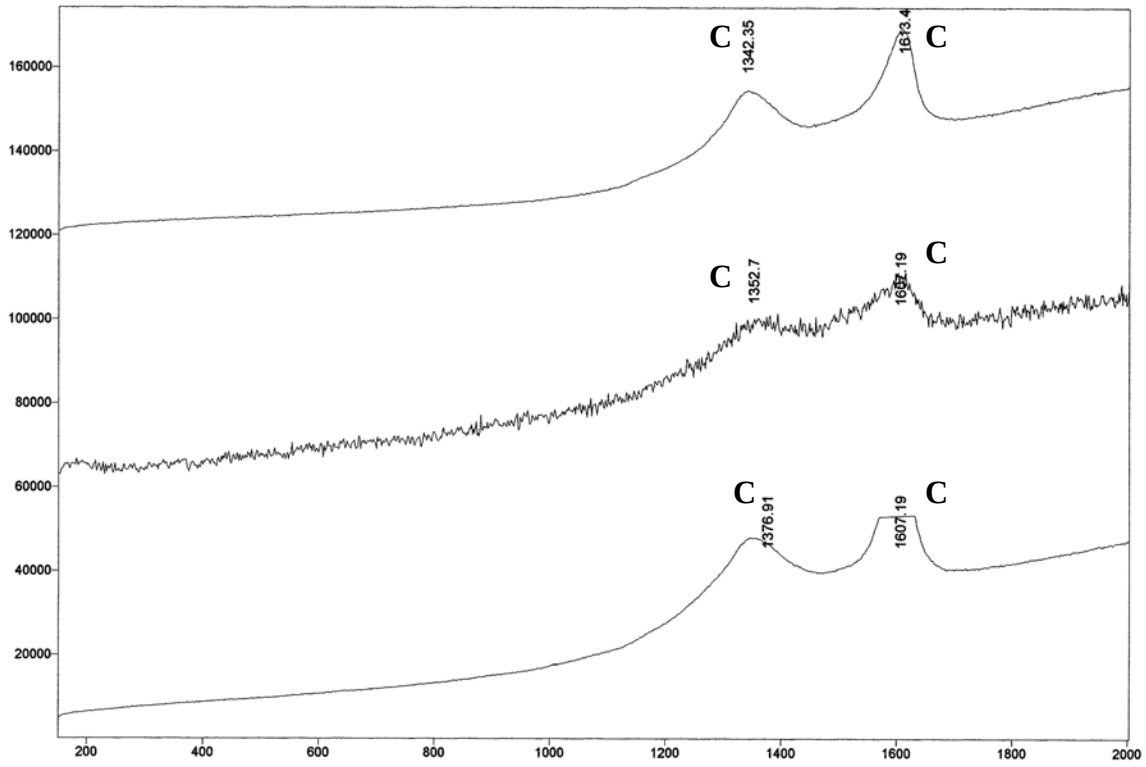

Figure 7: LRS for sample 2

Sample 3 consists of a Mo base structure that is 12.5 μm thick foil. It was run with 943 mL/min of Ar and 95 mL/min of H_2; after 120 seconds we shut off the H_2 and added 10 mL/min of C_2H_4 for 120 seconds. This is an identical procedure to sample 1, except using a foil sample. Then, the C_2H_4 flow was closed and the sample was run for 60 seconds more in only Ar gas. The voltage was 8.77 kV and the current was 75 mA.

Sample 4 is similar in procedure to sample 2, but instead used the 12.5 μm thick Mo foil. It was run with 943 mL/min of Ar and 95 mL/min of H_2 for 120 seconds. Immediately, 20.0 mL/min of C_2H_4 was added after closing the H_2 gas flow. This gas composition ran for 120 seconds, then the C_2H_4 flow was closed and the sample was kept for 60 seconds in the Ar flow alone. The voltage was 8.77 kV and the current was 75 mA.

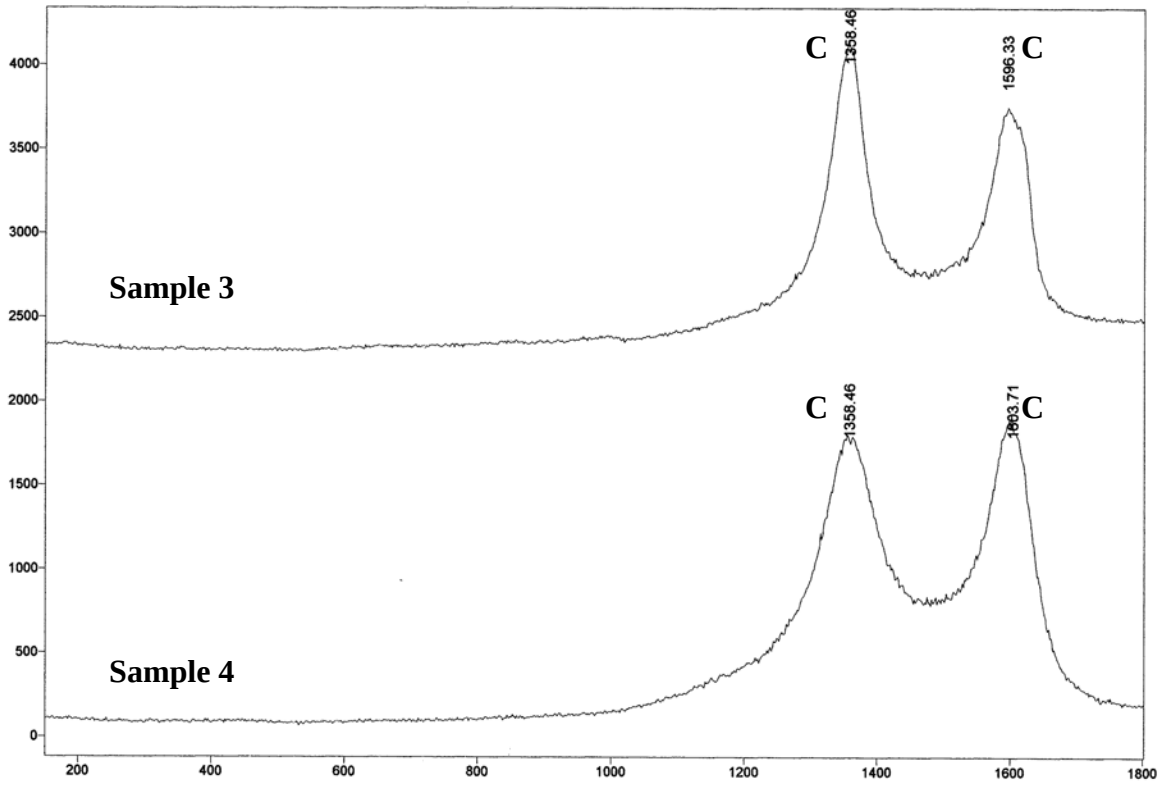

Figure 8: LRS for samples 3 and 4

Figure 8 represents the LRS of samples 3 and 4. During the analysis of the foil sample 3, we can see two peaks characteristic of a carbon-induced disorder. The first peak was at 1358.46 cm^{-1}, which is a disorder in the D-line[17, 28, 29]. The second peak was at 1596.33 cm^{-1}, which is caused by a G-line carbon disorder[28, 29]. As in the other samples, it is not possible to determine molybdenum oxide peaks with the Raman analysis. In addition, the analysis of sample 2 showed two main peaks at 1358.46 cm^{-1} and 1603.71 cm^{-1}. The first peak is caused by a carbon-induced disorder at the D-line[17, 28, 29], while the second peak is attributed to a G-line carbon disorder[28, 29]. It is not possible to determine any molybdenum oxide peaks in this sample using Raman.

8.2 XPS Spectra of Sample Surfaces and Analysis

This technique is based on the Einstein Photoelectric Effect. Incident x-rays cause emission of electrons from sample surface. The kinetic energy of the emitted electrons is measured and the difference between that energy and the monochromatic source gives a characteristic binding energy which is used to identify the composition[25]. We used a Kratos AXIS-165 Surface Analysis System with an aluminum x-ray source in using this technique.

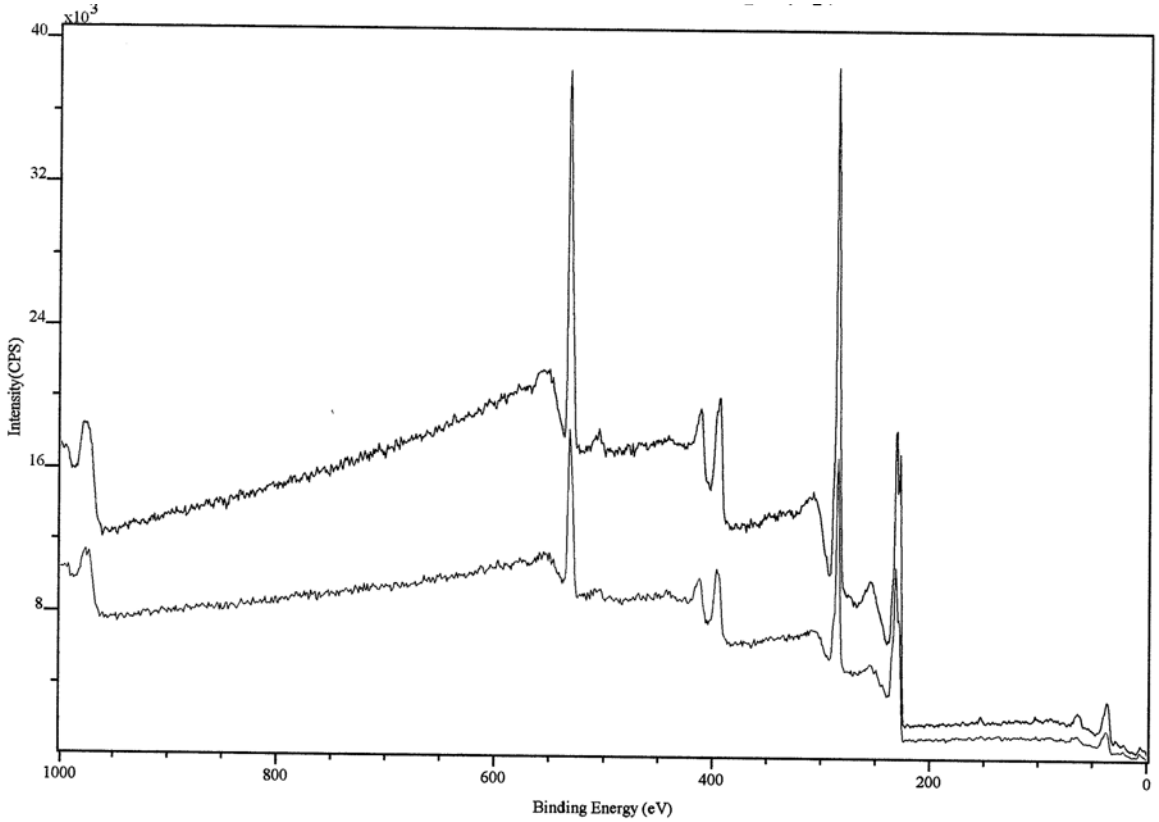

Figure 9: XPS survey for sample 1

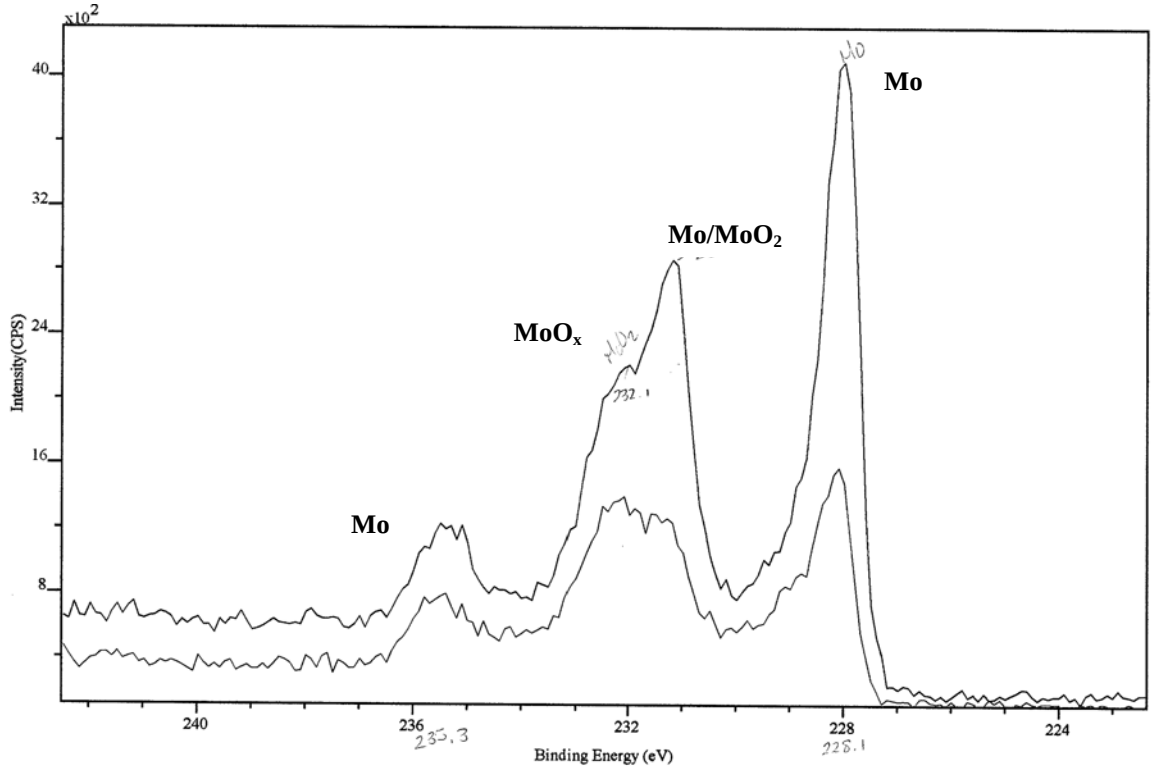

Figure 10: Mo 3d orbital in sample 1

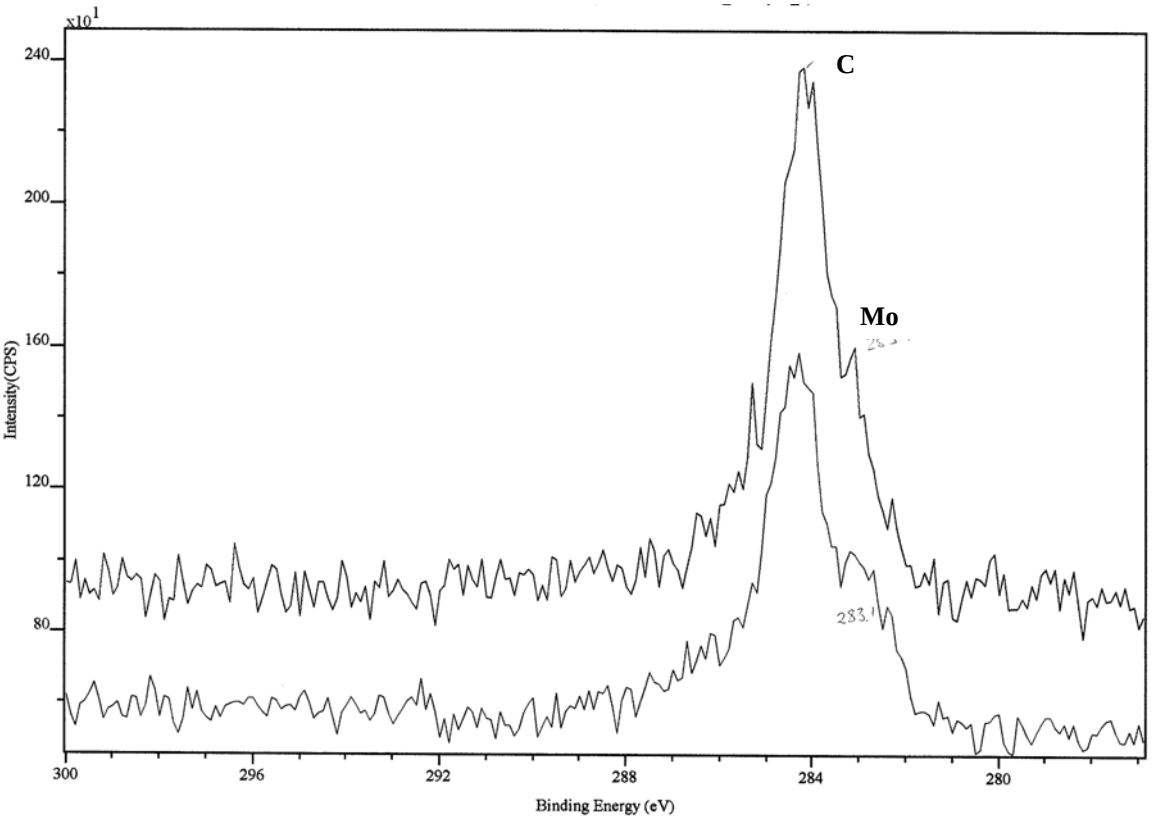

Figure 11: C 1s orbital in sample 1

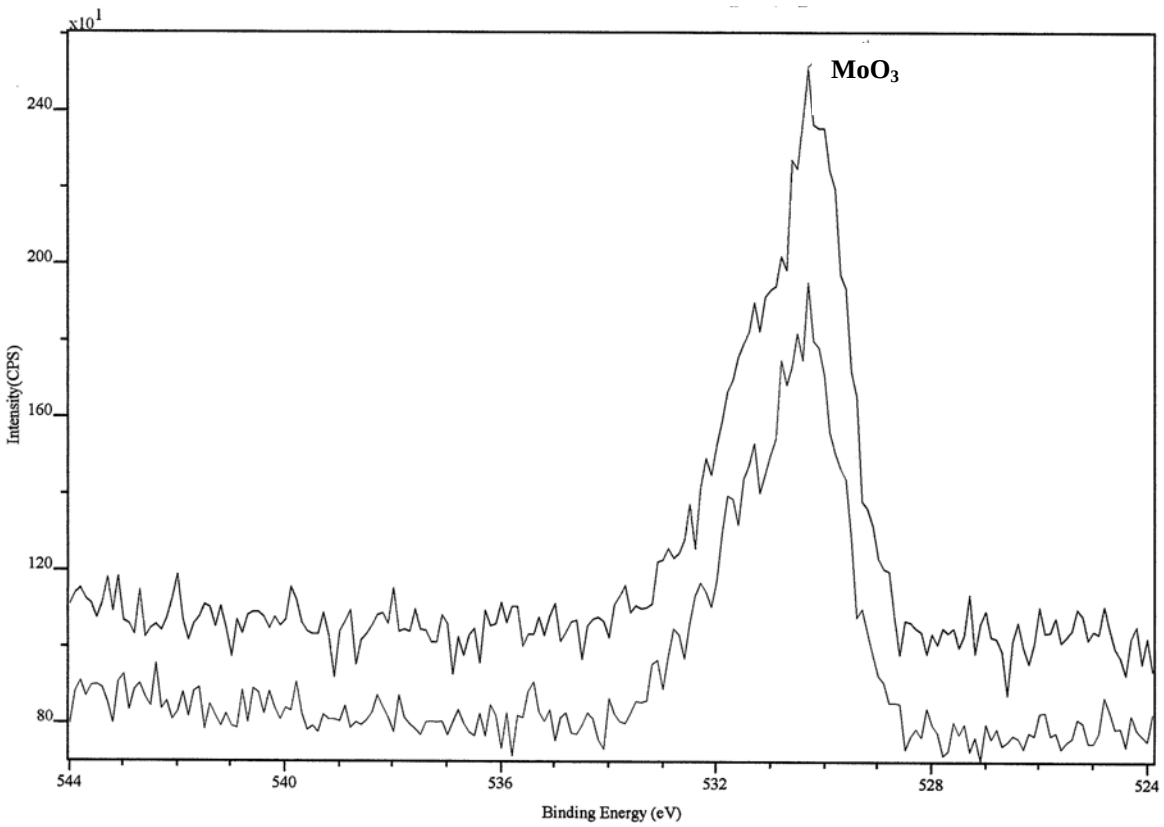

Figure 12: O 1s orbital in sample 1

Figure 9 showts a XPS survey of sample 1. Figures 10, 11, and 12 represent the regions of Mo 3d, C 1s, and O1s respectively of this sample. Figure 13 shows the XPS survey of sample 2. The Mo 3d orbital of sample 2 is shown in figure 14 as the C 1s and O 1s orbitals are represented by figures 15 and 16 correspondingly.

Table 1 shows the assignment of the peaks of samples 1 and 2. We can observe that sample 1 does not have any Mo_2C peaks, which suggest that a layer of carbide was not formed at the wire surface. On the other hand, sample 2 exhibits a peak at 282.6 eV, which is characteristic of Mo_2C[30] and implies that a carbide layer was formed at the surface of the wire. Both samples show peaks characteristic of carbon deposits as well as molybdenum oxides peaks in the O 1s orbital[19, 30]. Additionally, sample 2 has a peak at

286.4 eV characteristic of a C-O bond and a peak at 288.5 eV characteristic of a C=O bond[31].

Orbital	Sample 1	Assignment	Sample 2	Assignment
Mo 3d	228.1	Mo	----	Mo_2C
	231.2	Mo/MoO_2		
	232.1	MoOx		
C1s	283.1	Mo	282.6	Mo_2C
	284.3	C	284.8	C
			286.4	C-O
			288.5	C=O
O 1s	530.4	MoO_3	529.6	MoO_x
			530.8	MoO_x
			531.3	MoO_3

Table 1: XPS results for samples 1 and 2

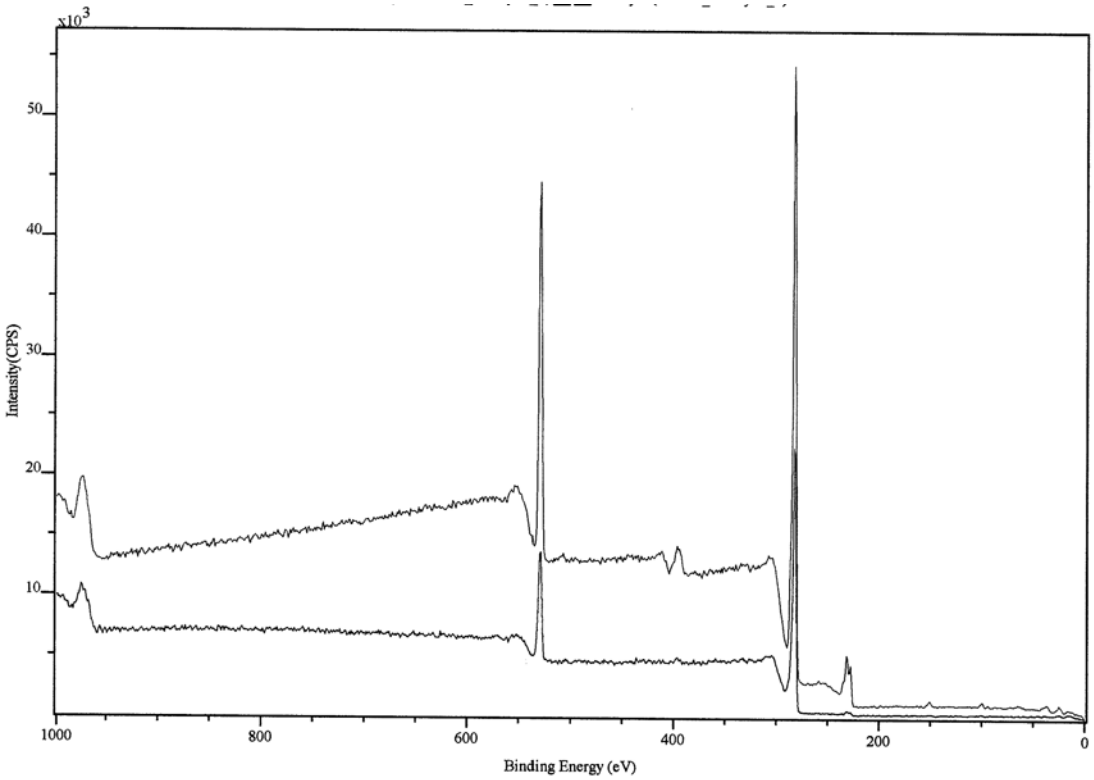

Figure 13: XPS survey for sample 2

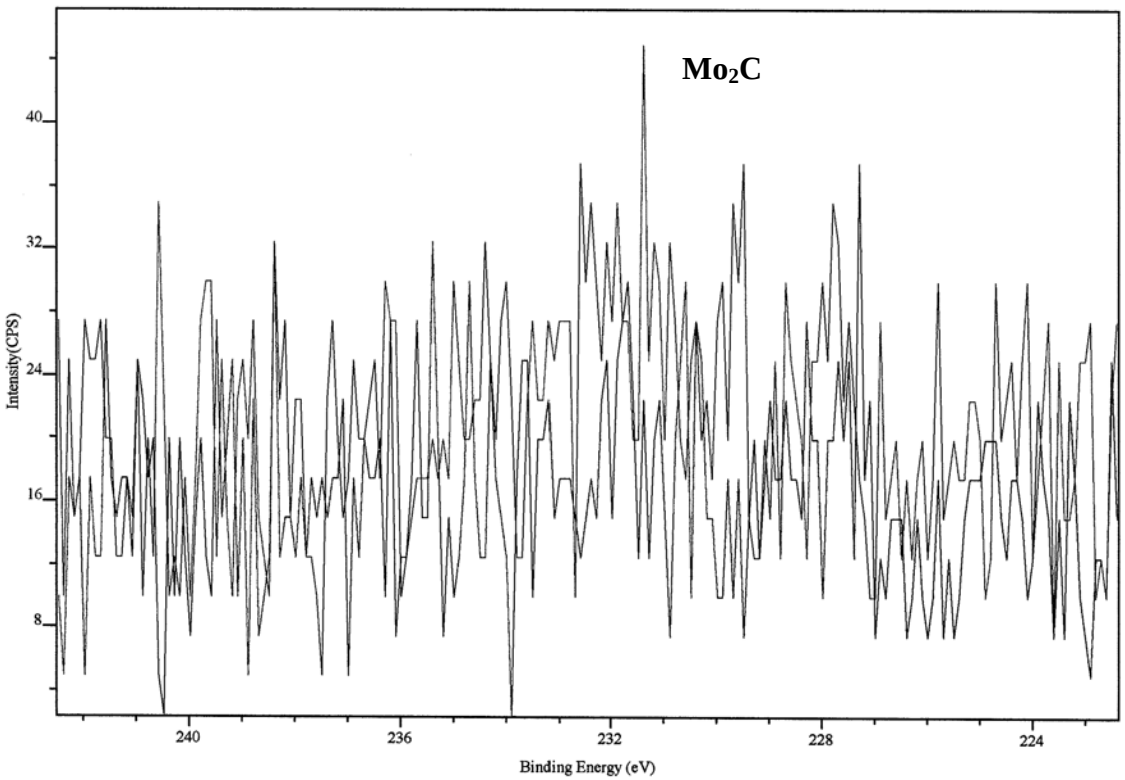

Figure 14: Mo 3d orbital in sample 2

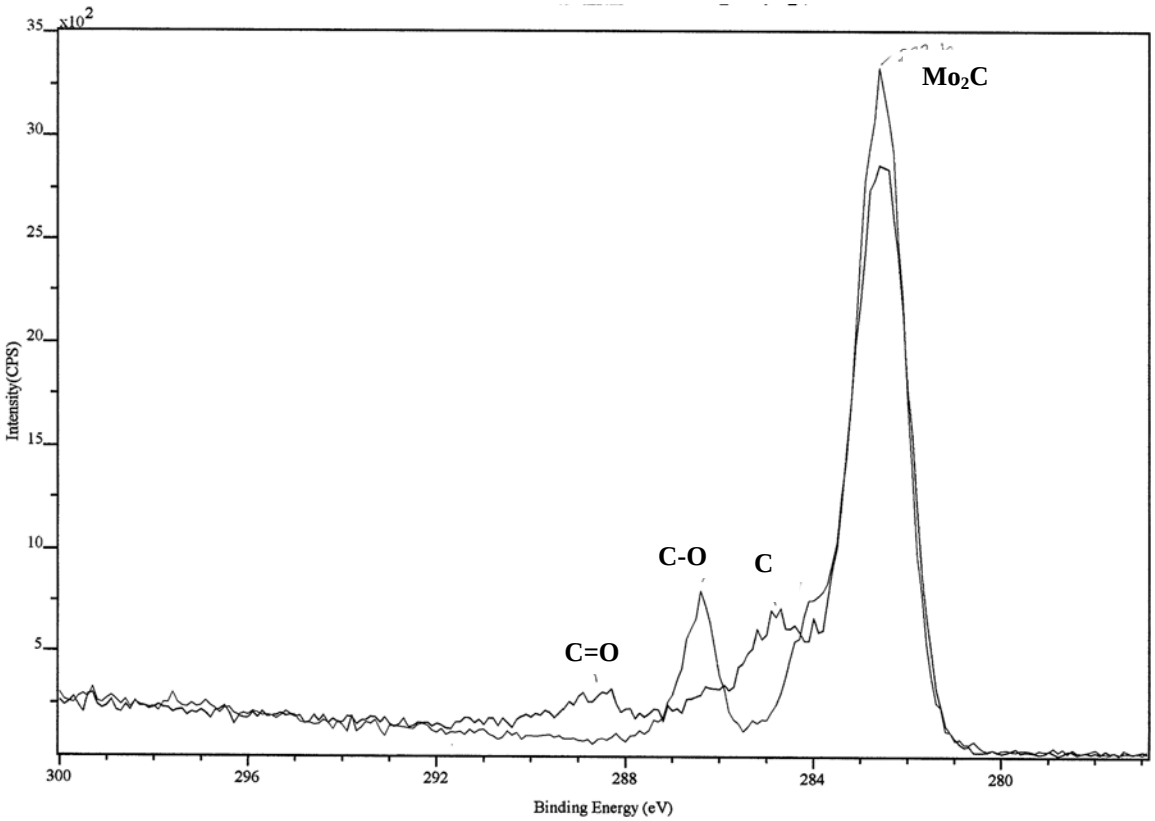

Figure 15: C 1s orbital in sample 2

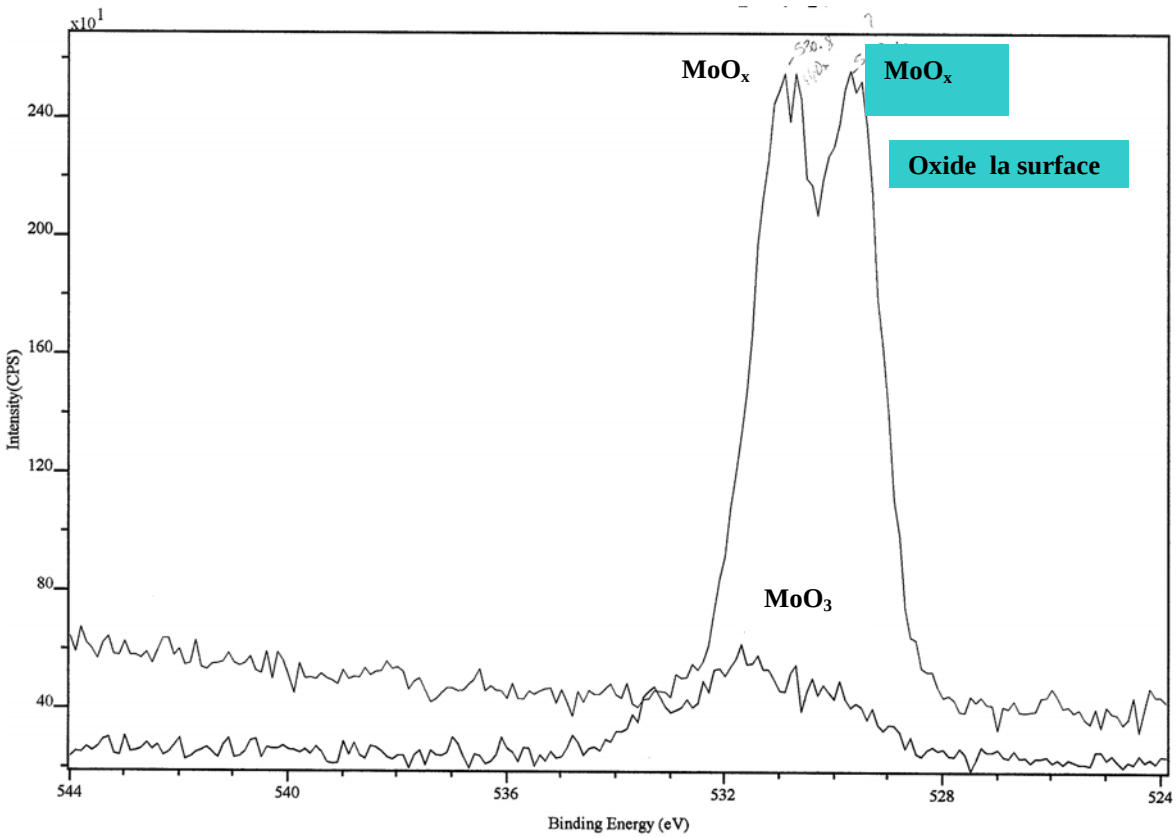

Figure 16: O 1s orbital in sample 2

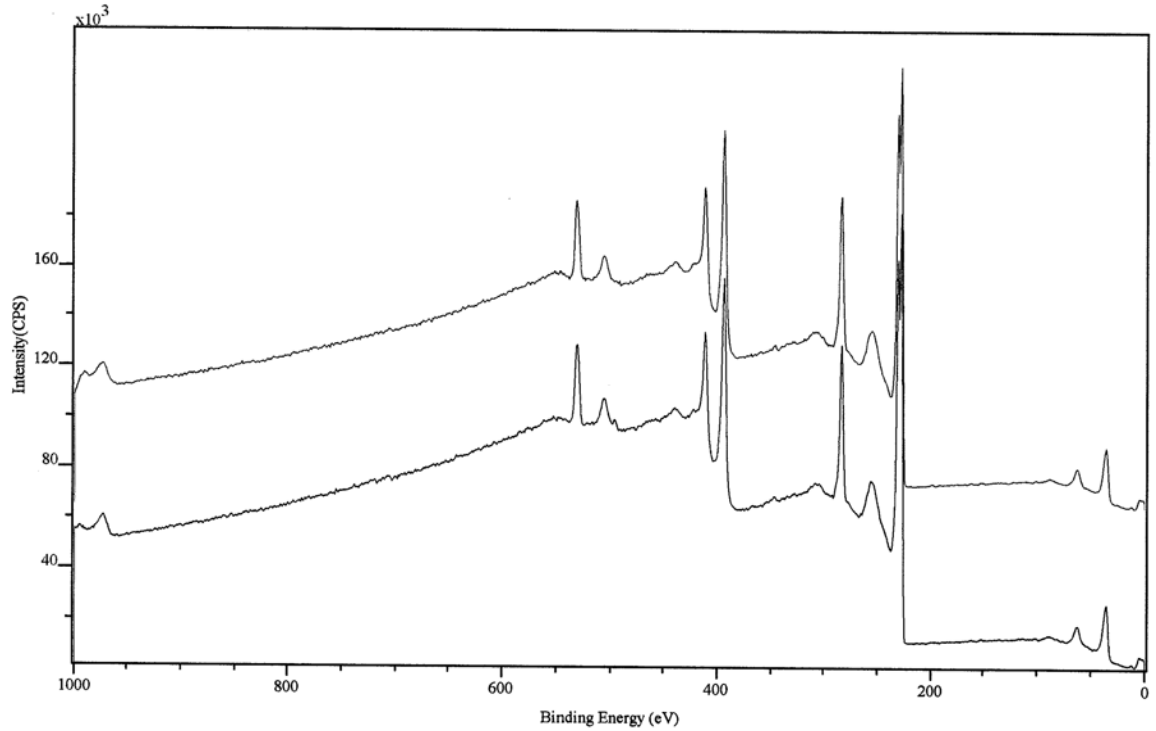

Figure 17: XPS survey for sample 3

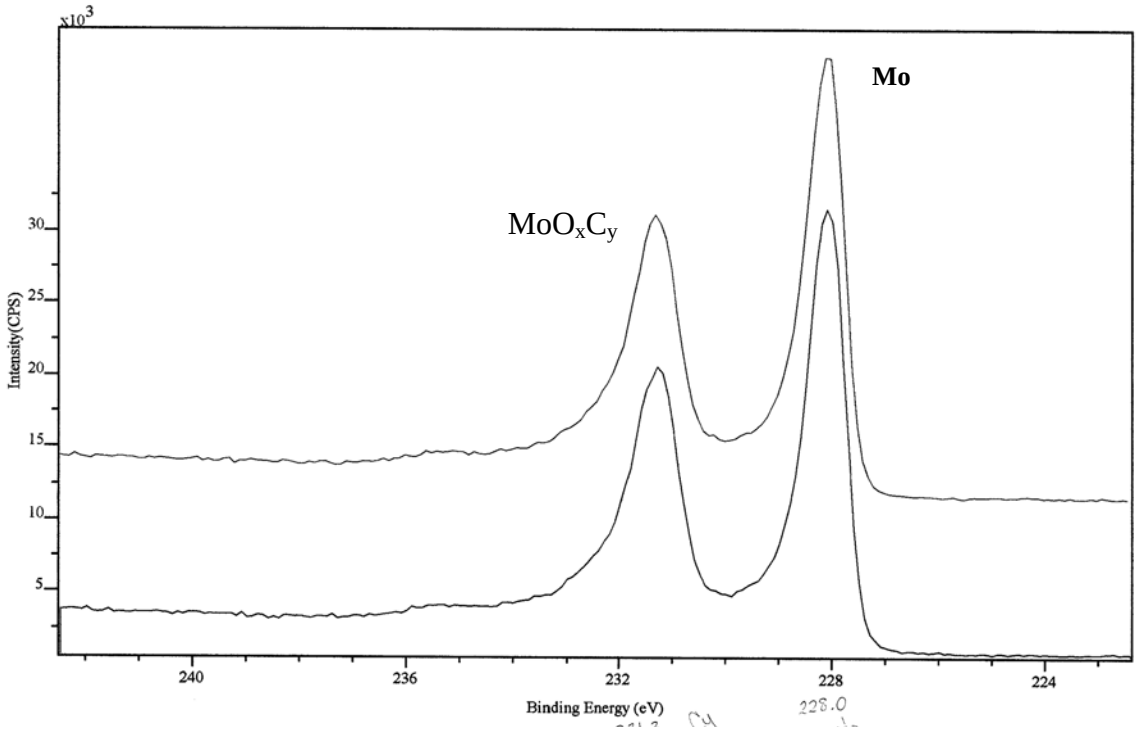

Figure 18: Mo 3d orbital in sample 3

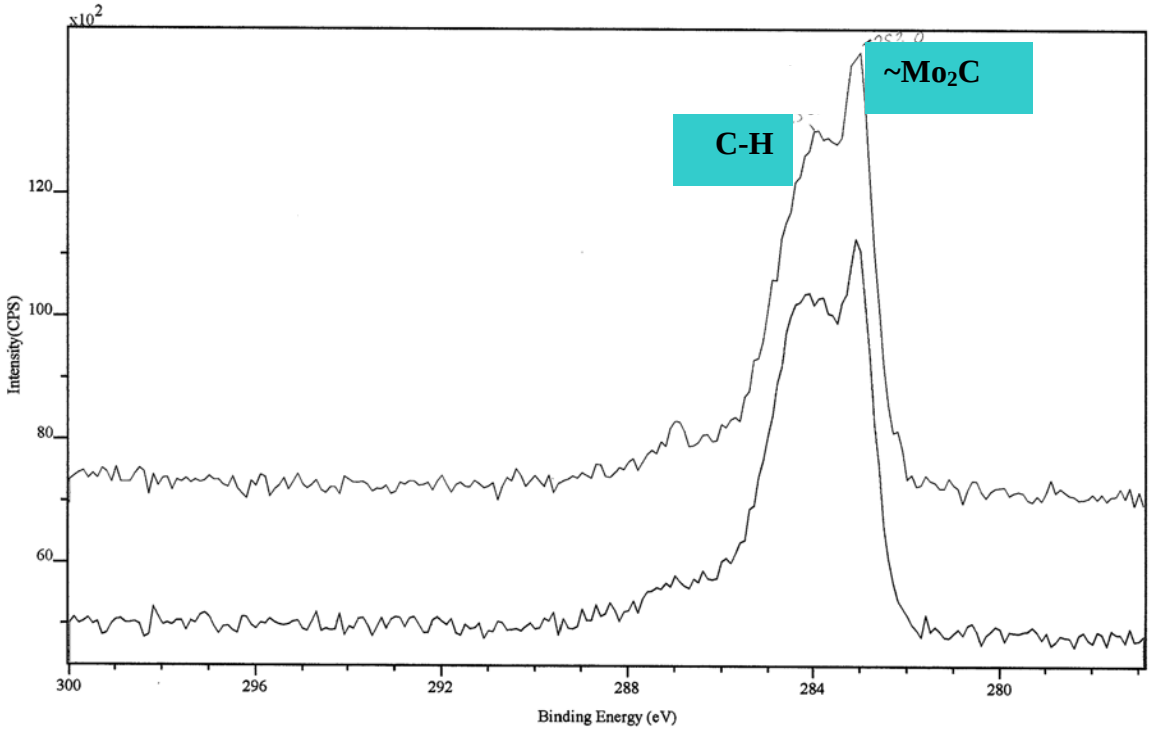

Figure 19: C 1s orbital in sample 3

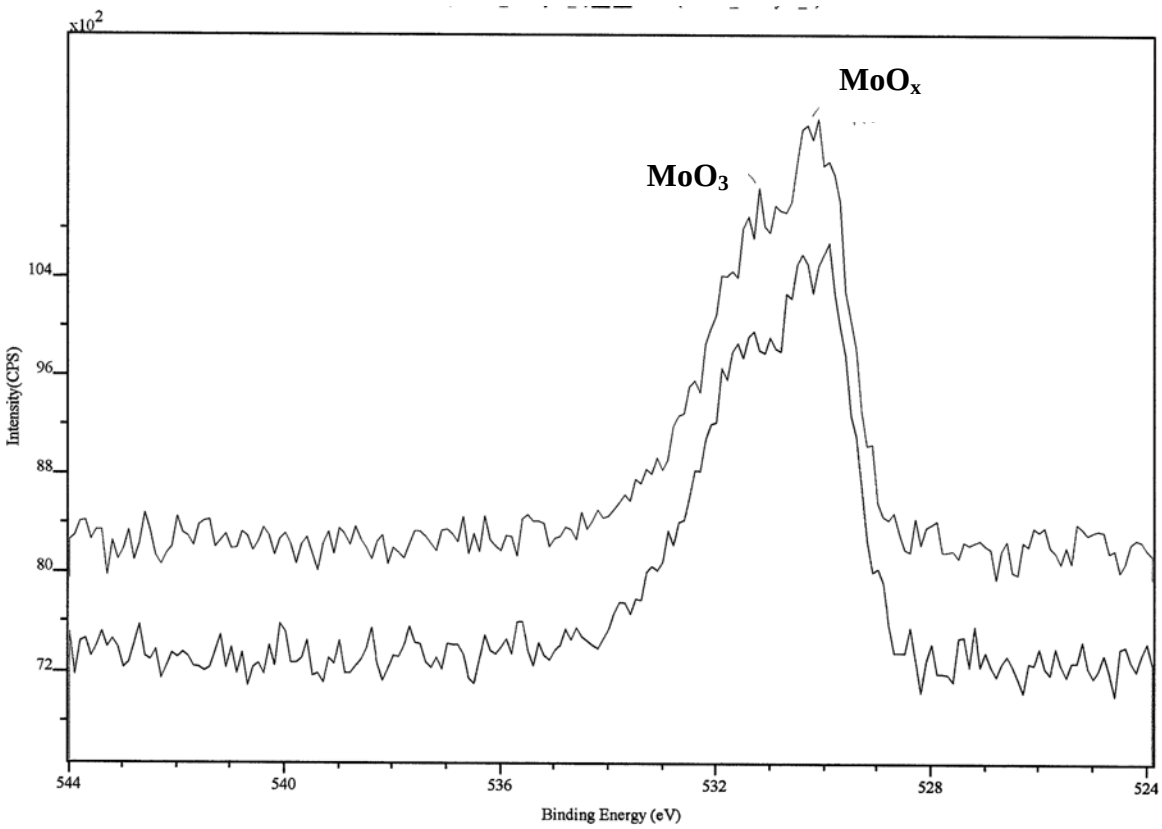

Figure 20: O 1s orbital in sample 3

Figure 17 represents a XPS survey of sample 3. Figures 18, 19, and 20 represent the Mo 3d, C 1s, and O 1s orbitals respectively. Figure 21 represents the XPS survey of sample 4. Mo 3d orbital of sample 4 is shown in Figure 22 as the C 1s and O 1s orbitals are represented by Figures 23 and 24 in that order. Table 2 contains the assignment of each peak of samples 3 and 4. Both samples show peaks characteristic of molybdenum oxides as well as carbon disorders[19, 30]. Sample 3 has a peak at 283 eV, characteristic of Mo_2C[32]. However, sample 4 has a peak at 227.8 eV[19, 30], which either could be Mo or Mo_2C. Sample 3 has a characteristic peak of molybdenum oxycarbide at 231.3 eV[7]. Sample 4 has a peak at 288.5 eV which could either be representative of a single or double bond between C and O.

Orbital	Sample 3	Assignment	Sample 4	Assignment
Mo 3d	228	Mo	227.8	Mo/ Mo_2C
	231.3	MoO_xC_y	232.1	MoO_3
			235.5	MoO_x
C 1s	283	Mo_2C	284.3	C
	283.9	C	288.5	C-O/C=O
O 1s	530.2	MoO_x	532.1	MoO_x
	531.3	MoO_3		

Table 2: XPS results for sample 3 and 4

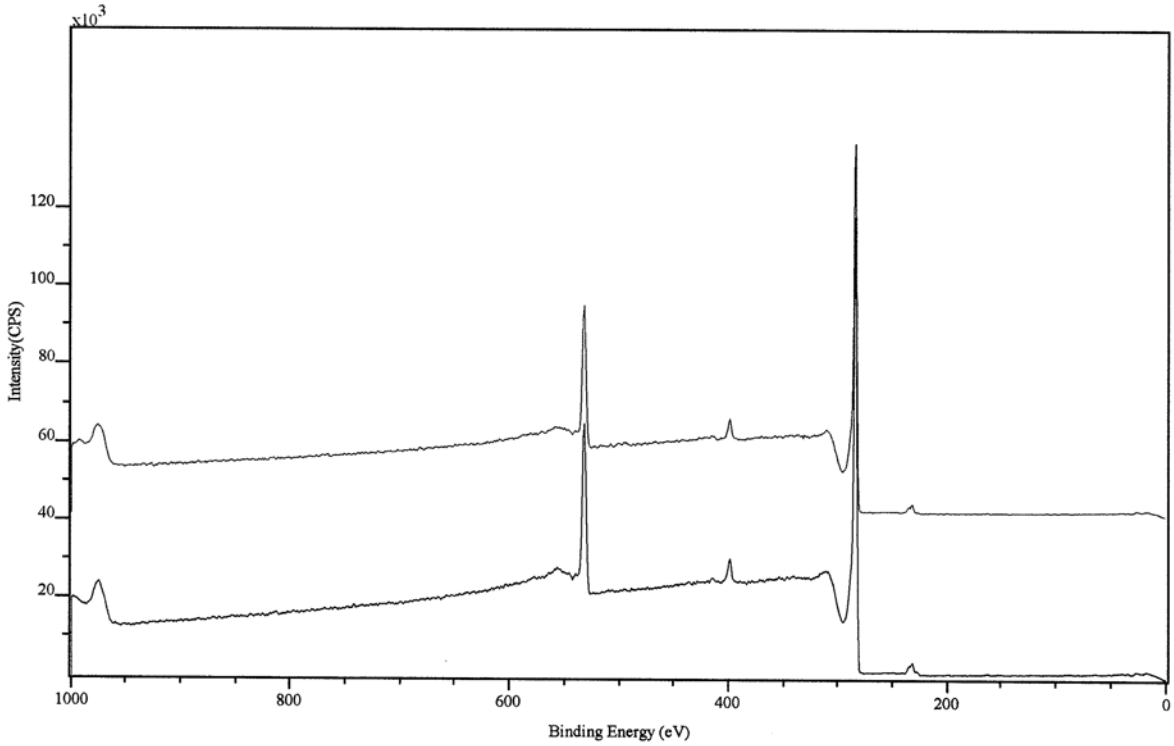

Figure 21: XPS survey for sample 4

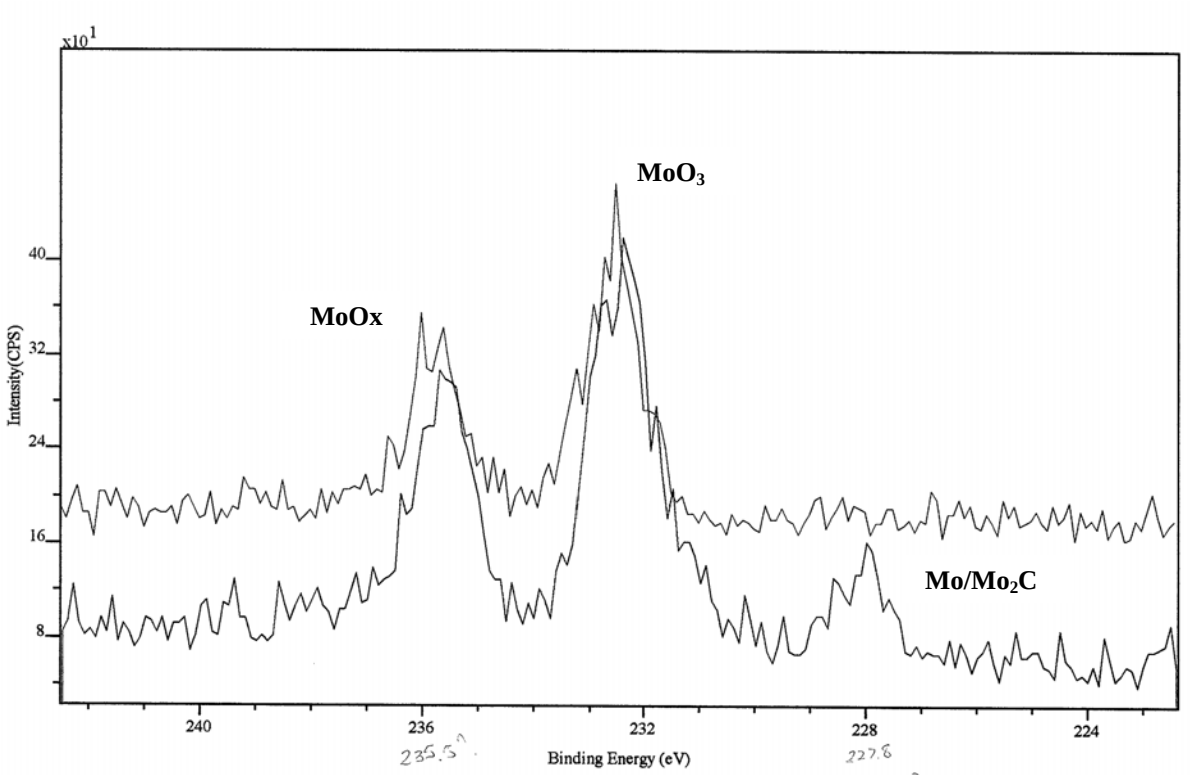

Figure 22: Mo 3d orbital in sample 4

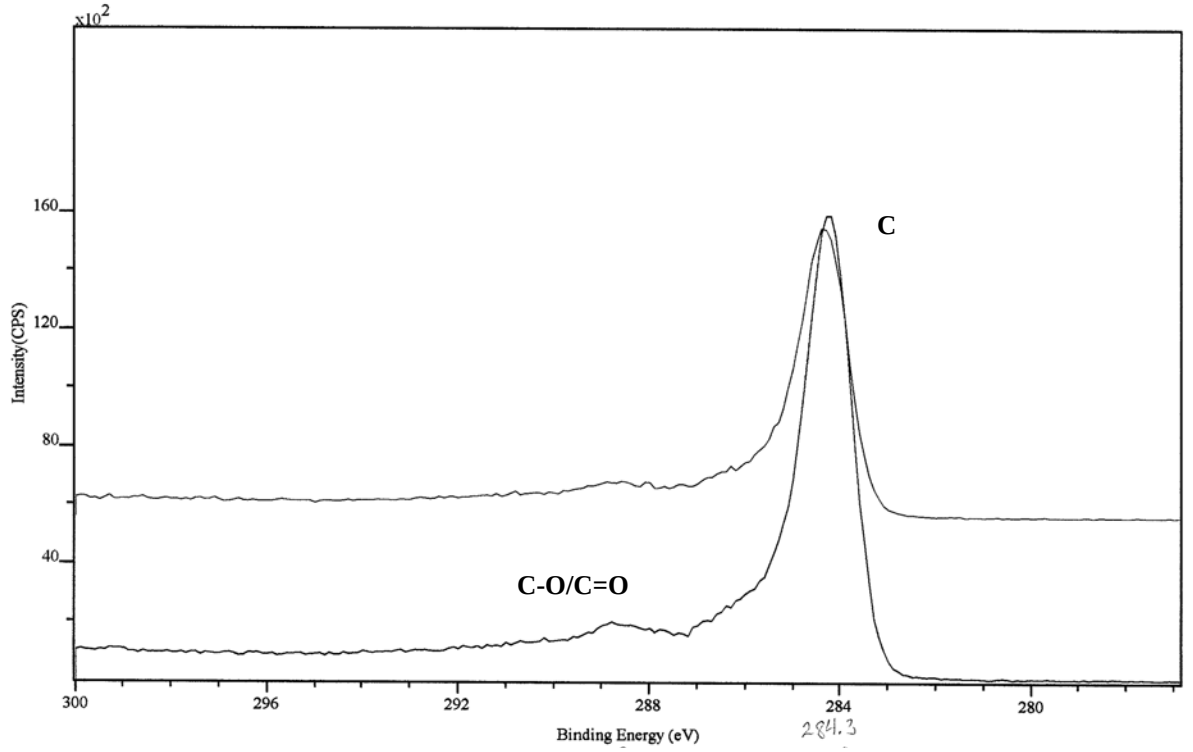

Figure 23: C 1s orbital in sample 4

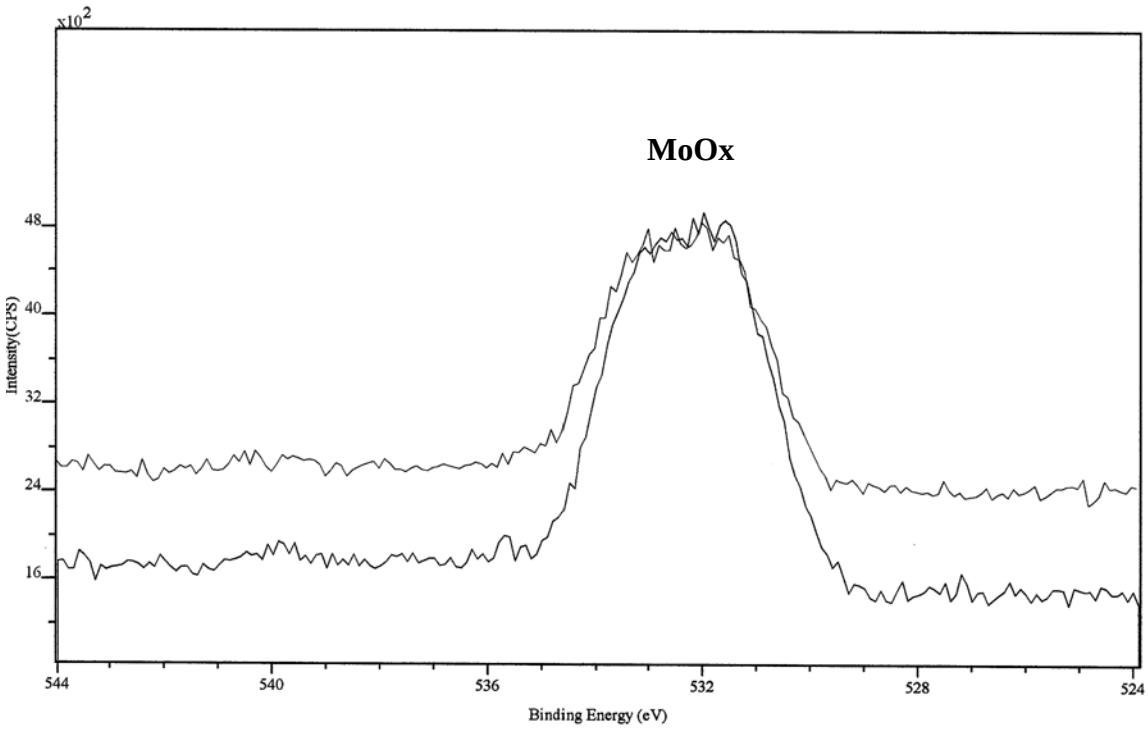

Figure 24: O 1s orbital in sample 4

8.3 SEM Analysis of the Sample Surfaces and Analysis

Secondary electrons, characteristic x-rays, and backscattered electrons are generated by an electron beam scanned across the sample surface. Detectors collect the signals to form images of the sample displayed on a cathode ray tube screen[20]. It is possible to see fractured surfaces and particulate materials with this tool. The instrument used here was a Hitachi S-3000N Variable Pressure SEM with an attached Oxford Inca EDS system.

To determine if the wire surface changed, the analysis of a standard of molybdenum wire was necessary to compare with the samples. Figures 25 and 26 show the surface of the Mo wire before the reaction. We see that the surface is not uniform and it has troughs along the surface. When we compare it with a sample run for 30 seconds in the reactor, seen in Figures 27 and 28, we observe that the surface of the sample is more uniform than the pure molybdenum wire. In addition, Figure 29 shows an end of the sample after it was cut with scissors and there are some layers of material that flaked off the Mo wire surface, further indicating the creation of a thin film.

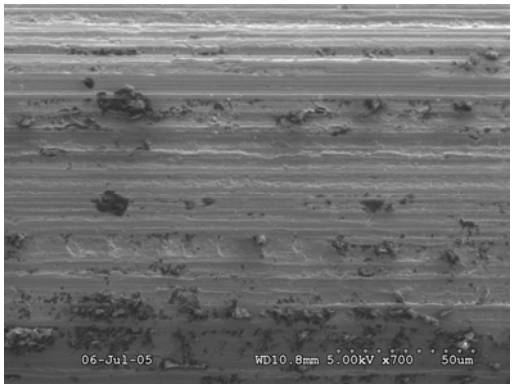

Figure 25: SEM of Mo wire reference at 700x and 5.00 kV.

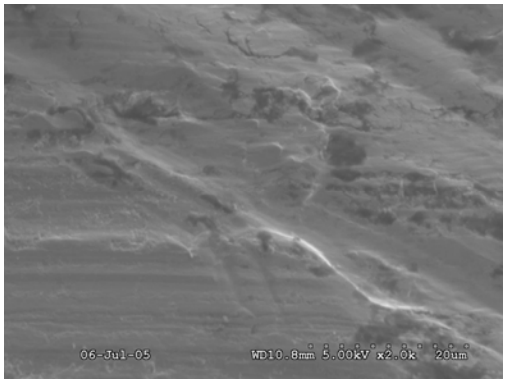

Figure 26: SEM of Mo wire reference at 2000x and 5.00 kV.

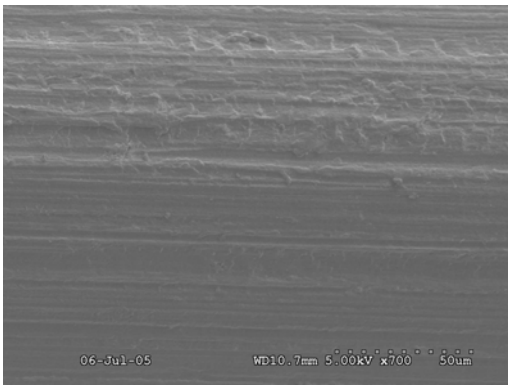

Figure 27: SEM of 30 second sample at 700x and 5.00kV.

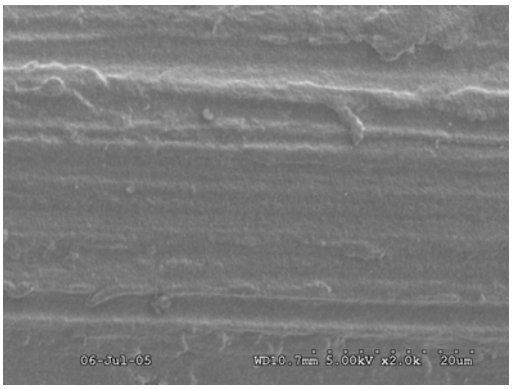

Figure 28: SEM of 30 second sample at 2000x and 5.00kV.

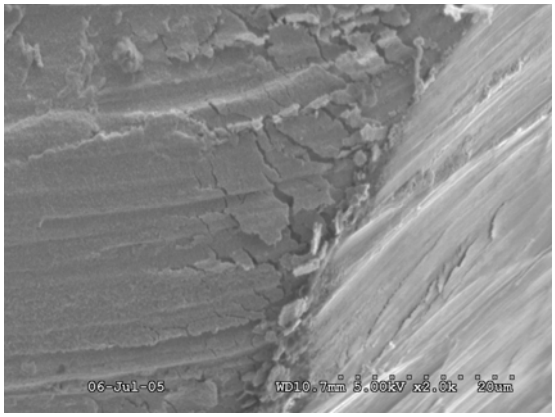

Figure 29: SEM of 30 second cut sample at 2000x and 5.00 kV

9.0 Conclusions and Future Research Proposed

SEM images have confirmed that the plasma-assisted reaction is creating surface changes on the molybdenum. Irregularities on the surface are lessened, indicating that a film has been deposited. However, XPS and Raman spectra data indicate a variance of the film composition with several possible components. Analysis suggests that carbon deposits and molybdenum oxides are forming during the reaction in addition to the molybdenum carbide and possibly an oxycarbide as well. All of these surface species are materializing across samples in a non-uniform composition.

The experimental parameters of time, gas phase composition and gas phase pressure all appeared to have an effect on the uniformity and chemical make-up of the induced film. If sufficient reaction time was not permitted, we observed a low yield of reactant species and the molybdenum remained unaltered. However, extended reaction times resulted in the creation of large amounts of carbon deposits and oxide species. We observed this same relationship when varying the gas phase composition. If the concentration of ethylene was minimal, the only alterations on the molybdenum surface were oxides. Conversely, when the concentrations of ethylene gas were high, excessive carbon deposits were generated.

Variations with pressure revealed a similar trend: increased pressure resulted in greater concentrations of reactive species. If the pressure was set too low, film formation did not occur. However, if the pressure is increased beyond some threshold, the carbide film could be burned off and the molybdenum sample melted altogether.

The observed variations indicated that optimal values do exist to allow for film formations that do not include large deposits of unwanted material such as oxides and carbon graphite structures. Molybdenum oxides and carbon deposits indicate that surface modifications are taking place, which are essential to the formation of carbide films.

The availability of diagnostic tools prevented us from definitively distinguishing the presence of molybdenum carbide. We believe that Transmission Electron Spectroscopy (TEM) could be used to measure the crystal structure d-spacing, which could then be compared with known results in the literature. In concurrence with our research, this future work should confirm the film's components.

Finally, a process for the synthesis of catalysts in powder form also requires additional investigation. These powders are needed in order to test for the catalytic activity of the molybdenum carbide via the Water-Gas Shift Reaction. Constructing a reactor to allow fluidization of metal particles during the plasma process will be essential to this final characterization of the catalyst so that we can achieve even film formation. Designing this element and applying the knowledge of controlling reactor parameters from previous experiments will determine the industrial significance of this plasma-assisted process.

10.0 References

1. York, Andrew. "Magic Catalysts." Chemistry in Britain. 55 (1999): 25-27.
2. Chen, J.G. "Carbide and Nitride Overlayers on Early Transition Metal Surfaces: Preparation, Characterization, and Reactivities." Chemical Reviews. 96 (1996): 1477-1498.
3. Li, Y. Z., et al. "Selective Liquid Hydrogenation of Long Chain Linear Alkadienes on Molybdenum Nitride and Carbide Modified by Oxygen." Chemical Engineering Journal. 99 (2004): 213-218.
4. Iyer, M. V., et al. "Catalysis for Synthesis Gas Formation from Reforming of Methane. Topics in Catalysis. 29 (2004): 197-200.
5. Ledoux, M. F., C. Pham-Huu, and R. Chianelli. "Catalysis with Carbides." Current Opinion in Solid State & Materials Science. 1 (1996): 96-100.
6. Patt, J., et al. "Molybdenum Carbide Catalysts for Water-Gas Shift." Catalysis Letters. 65 (2000): 193-195.
7. Moon, D. J., and J. W. Ryu. "Molybdenum Carbide Water-Gas Shift Catalyst for Fuel Cell-Powered Vehicles Applications." Catalysis Letters. 92 (2004): 17-24.
8. Costa, P. Da, et al. "Deep Hydrodesulphurization and Hydrogenation of Diesel Fuels on Alumina-Supported and Bulk Molybdenum Carbide Catalysts." Fuel. 83 (2004): 1717-1726.
9. Furmisky, E. "Metal Carbides and Nitrides as Potential Catalysts for Hydroprocessing." Applied Catalysis A: General. 240 (2003): 1-28.
10. Bej, S. K., and L. T. Thompson. "Acetone Condensation Over Molybdenum Nitride and Carbide Catalysts." Applied Catalysis A: General. 264 (2004): 141-150.
11. Bender, J., J. Dunn, and K. Brezinsky. "Microwave-Assisted Synthesis of Carbide and Nitride Nanolayers on Transition Metals." In the Science and Engineering of Catalyst Preparation. Ed. J. Regalbuto. New York: Marcel Dekker, 2005.
12. White, C. L. Plasma Assisted Binder Burnout of Ceramic Materials. Chicago: University of Illinois at Chicago, 1999.
13. Cote, D. R., et al. "Plasma-Assisted Chemical Vapor Deposition of Dielectric Thin Films for ULSI Semiconductor Circuits." Journal of Research and Development. 43 (1999): 5-38.
14. Craig, A., et al. "Modification of Inert Surfaces by PECVD and Their Characterization by Surface Analysis Techniques." Poster Presentation at Biointerface 2003. 22-24 Oct. 2003. Savannah, GA.
15. Saveliev, A. Personal Interview. 6 July 2005.
16. Clark, George L. The Encyclopedia of Spectroscopy. New York: Reinhold Publishing Corporation, 1960.
17. Xiao, T., et al. "Study of the Preparation and Catalytic Performance of Molybdenum Carbide Catalysts Prepared with C_2H_2/H_2 Carburizing Mixture." Journal of Catalysis. 211 (2002): 183-191.

18. Di Giuseppe, G. and J. Robert Selman. "Thin film deposition of Mo and Mo-compounds by PECVD from $Mo(CO)_6$ and MoF_6 as precursors: characterization of films and thermodynamic analysis." Journal of Electroanalytical Chemistry. 559 (2003): 31-43.
19. La Surface.com. Benoit, R. 2005. Thermo Electron Corporation. 28 June 2005. <http://www.lasurface.com/database/elementxps.php>.
20. Scanning Electron Microscopy & Field Emission Scanning Electron Microscopy. The Advanced Materials Research Institute. 9 July 2005. <http://www.amri.uno.edu/wzhou/scanning_electron_microscope.htm>.
21. Mattox, Donald M. "Applications of Vacuum Coating." The Society of Vacuum Coaters. 2005. <http://www.svc.org/AboutSVC/AS_AppsofVac.html>.
22. Oyama, S. T. "Preparation and Catalytic Properties of Transition Metal Carbides and Nitrides." Catalysis Today. 15 (1992): 179-200.
23. Neylon, M.K., et. al. "Ethanol amination catalysis over early transition metal nitrides." Applied Catalysis A: General. 232 (2002): 13-21.
24. Tsuchida, T. and T. Kakuta. "Synthesis of NbC and NbN_2 by MA-SHS in air process." Journal of Alloys and Compounds. 398 (2005): 67-73.
25. Surface Analysis Forum. Simon Morton. 1998. 24 February 2001. <http://www.uksaf.org/tech/xps.html>.
26. Xiao, T., et. al. "Preparation of Molybdenum Carbides Using Butane and Their Catalytic Performance." Chemistry of Materials. 12 (2000): 3896-3905.
27. Xiao, T., et. al. "Effect of sulfur on the performance of molybdenum carbide catalysts for the partial oxidation of methane to synthesis gas." Catalysis Letters. 83 (2002): 241-246.
28. Gupta, S., et al. "Ultraviolet and Raman Spectroscopic investigations of nanocrystalline carbon thin films grown by bias-assisted hot filament chemical vapor deposition." Journal of Raman Spectroscopy. 34(2003): 192-198.
29. Gupta, S., et al. "Ex-situ spectroscopic ellipsometry and Raman Spectroscopy investigations of chemical vapor deposited sulfur incorporated nanocomposite carbon thin films." Thin Solid Films. 455-456 (2004): 422-428.
30. http://www.nist.gov/srd/nist20.htm
31. Delporte, P., et al. "Physical Characterization of molybdenum oxycarbide catalyst; TEM, XRD and XPS." Catalysis Today. 23 (1995): 251-267
32. Miyao, T., "Preparation and characterization of alumina-supported molybdenum carbide." Applied Catalysis A: General. 165 (1997): 419-428
33.